REF: A0735. 0708

THERMAL BEHAVIOR AND PERFORMANCE CHARACTERISTICS OF A TWIN AXIAL GROOVE JOURNAL BEARING AS A FUNCTION OF APPLIED LOAD AND ROTATIONAL SPEED

F.P. Brito[1*], J. Bouyer[2], M. Fillon[2], and A.S. Miranda[1]
[1]Universidade do Minho, Departamento de Engenharia Mecânica, Guimarães, Portugal
[2]Université de Poitiers, Laboratoire de Mécanique des Solides, Poitiers, France
Email: [(*)]francisco@dem.uminho.pt

SYNOPSIS

An experimental investigation of the influence of applied load and rotational speed on the performance of a 100mm diameter plain journal bearing with two axial grooves located at ±90º to the load line has been carried out. The applied load varied from 2 to 10kN, whereas the rotational speed ranged from 1000 to 4000 rpm.

Measurements of hydrodynamic pressure, temperature profiles at the oil-bush and oil-shaft interfaces, oil flowrate and minimum film thickness under steady state conditions have been performed and the results discussed.

The operating conditions were found to affect significantly the temperature profile inside the bearing. At low eccentricity tests the maximum temperature occurred at the unloaded lobe of the bearing, with the downstream groove contributing poorly to bearing cooling. As eccentricity increased, a temperature increase in the loaded lobe of the bearing was observed, along with a temperature decrease in the unloaded lobe. At high eccentricities the downstream groove was found to contribute significantly to bearing cooling. Shaft temperature and oil outlet temperature did not seem to be significantly affected by increasing load.

INTRODUCTION

Journal bearings are widely used in rotating machinery, especially when shafts are submitted to both high speeds and heavy applied loads. Bearing thermal behavior and its effect on performance has been studied since several decades from now. In order to estimate bearing performance taking into account thermal effects, thermohydrodynamic (THD) theoretical models were developed focusing mainly on the single axial groove bearing geometry (Boncompain et. al, 1986, Mitsui, 1987, Pierre et. al, 2000). Existing theoretical models for twin groove bearings (Knight & Ghadimi, 1992, Ma & Taylor, 1994) still do not fully predict the thermal behavior of the bearing. The existence of an additional groove dramatically affects flow patterns and temperature profiles inside the bearing. It is still not fully understood the role of each oil supply groove on bearing cooling for different operating conditions.

Experimental data is essential to fully understand the bearing behavior and to improve theoretical modeling. It is worth mentioning the experimental works of Lund & Tonnesen (1984), Fitzgerald & Neal (1992) and Ma & Taylor (1995) on twin axial groove journal bearings. The available experimental data concerning this bearing geometry is still rather limited. The present work aims to address this lack of information, presenting and discussing experimental results obtained for a span of operating conditions that include the less studied

cases, like, for instance, the lightly loaded bearing. Although of limited practical applicability, these results are useful for a correct understanding of the bearing behavior.

EXPERIMENTAL PROCEDURE

Figure 1(a) represents the bearing test rig of the *Laboratoire de Mecanique des Solides* (LMS) which has been used for the present work. A table displaying the operating conditions, the geometric parameters and the lubricant properties used in the tests is presented in Fig.1(b). Only a brief description of the experimental layout will be given here, since several experimental studies from that of Ferron et al.(1983) to the recent work of Bouyer and Fillon (2002), have been performed using this installation. A detailed description of the experimental layout can be found in these studies.

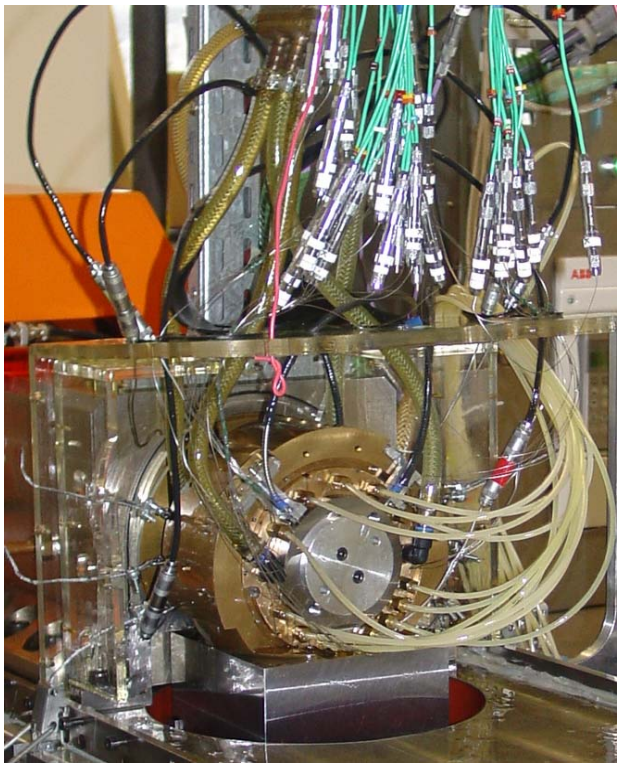

Parameters		**Units**	**Value/Span**
Rotational speed	N	rpm	1000, 2000, 3000, 4000
Applied load	W	kN	2, 4, 6, 8, 10
Supply pressure	P_f	kPa	140
Supply temperature	T_f	ºC	40
Bush inner diameter (nominal)	d	mm	100
Bush outer diameter (including sleeve)	D	mm	200
Bush length	b	mm	80
Groove length	a	mm	70
Circumferential extension of each groove	w	mm	16
Diametral clearance (20ºC)	C_d	µm	171
Lubricant viscosity (40ºC)	μ_{40}	Pa.s	0.0293
Lubricant viscosity (70ºC)	μ_{70}	Pa.s	0.0111
Lubricant thermal conductivity	K_l	W/mK	0.13
Bush thermal conductivity	K_b	W/mK	50
Lubricant specific mass	ρ	kg/m^3	870
Lubricant specific heat	Cp	J/kgK	2000
Ambient temperature (inside protection box)	T_{amb}	ºC	32 to 47

(a) (b)

Figure 1 – (a) Bearing Test Rig; (b) operating conditions, bearing geometry and lubricant properties

Shaft speed, applied load and oil supply conditions such as oil supply pressure and supply temperature, can be controlled. The measured parameters were the following: oil flowrate, temperature fields at the oil-bush and oil-shaft interfaces, oil outlet temperature, bush body temperature at different locations, minimum film thickness and hydrodynamic pressure along the mid-plane of the inner surface of the bush. An outline of the bearing under operation is presented in Fig. 2(a).

The shaft is driven by a 21kW variable speed DC motor via a transmission belt. The speed is regulated by an electronic controller with an accuracy of ±5 rpm. Three precision pre-loaded rolling bearings support the shaft, providing a stable and stiff mode of operation for the system.

The inner part of the bush, depicted in Fig. 2(b), is made of bronze and is designed to be inserted in a pre-existent sleeve whose purpose is to permit the testing of different bush geometries in the same experimental machine. The shaft is made of 100C6 steel.

The loading system relies on a pneumatic cylinder that acts on the bearing body. The load is applied to the bush along the vertical direction. Between the loading system and the test bearing there are two hydrostatic bearings, one being spherical and the other flat. These ensure that the load is applied to the bush body without parasitic torques.

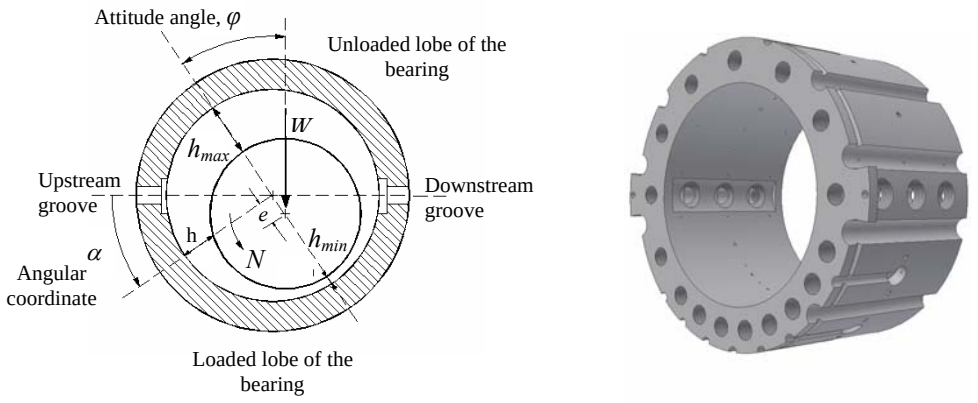

(a) (b)

Figure 2 – (a) Outline of the bearing under operation, (b) 3D drawing of the inner part of the bush

The feeding pressure is regulated by a precision restrictor valve. This parameter is monitored by a Bourdon type pressure gauge located at the oil distribution collector. The supply temperature is regulated via a cryothermostat serving the oil tank. Its value is monitored by a thermocouple located in the oil distribution collector and is kept within a range of ±1ºC from the set point.

In order to carry out the measurements under a steady-state regime, start-up times were set for thermal stabilization. Between tests, parameters such as temperature and flow-rate were monitored until stabilization occurred.

Oil flowrate was measured by a gear flow meter with an accuracy of ±0.05 l/min, attached to the data acquisition.

The temperature field was monitored by type K thermocouples, inserted in 0.5mm diameter metal sleeves and attached to a data acquisition system. The accuracy of the measurements is ±0.7ºC. The temperature at the bush-film interface was measured at the locations depicted in Fig. 3. The sleeved thermocouples were placed inside fully drilled holes, with the active part of the thermocouple being flush with the inner surface of the bush. Furthermore, thermocouples were positioned so as to measure the oil outlet temperature, the ambient temperature (environment temperature around the bearing) and the bush body temperature at two different locations. The shaft-film interface temperature was also measured at three different points by type K thermocouples connected to the system by a mercury rotary joint.

The hydrodynamic pressure distribution along the mid-plane of the bearing was measured via several Bourdon type pressure gauges attached via manifold valves to a series of 1mm holes drilled in the bush mid-plane at the locations depicted on Fig. 3.The measured pressure was generally greater than 30% of the total range of each pressure gauge. The measuring

uncertainties are ±0.01MPa for pressure values lower than 0.1MPa, and ±3% for higher values.

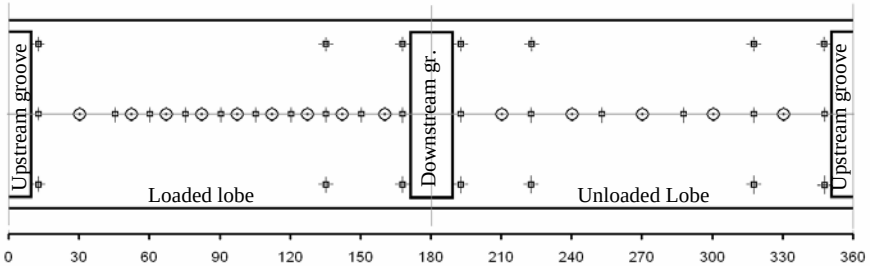

Figure 3 – location of the thermocouples (⌖) and pressure holes (⊙) at the inner surface of the bush.

Minimum film thickness was calculated from the output of two pairs of Eddy current proximity probes located at ±45º in relation to the load line, on both sides of the bearing. The sensitivity of each sensor ranges from 7 to 7.63mV/μm. The accuracy of the displacement measurements was ±5μm. The proximity measurements were corrected taking into consideration the estimated thermal deformation of the system. For each rotational speed, the locus of the shaft center was relative to a reference test, where the absolute position of the shaft has been obtained from a theoretical model. The tests chosen as reference were those with a load of 6kN, which is the middle range load.

In order to check measurements repeatability, each test was repeated at least once on a different occasion. Differences in maximum pressure and maximum temperature were in most cases less than ±0.01MPa and ±1ºC, respectively.

RESULTS AND DISCUSSION

Results concerning hydrodynamic pressure distribution at the mid-plane of the bearing, minimum film thickness, oil flowrate, temperature profiles at the oil-bush and oil-shaft interfaces, and oil outlet temperature will be presented and discussed.

The load varied from 2 to 10kN in 2kN intervals while the rotational speed varied from 1000 to 4000 rpm in 1000rpm intervals. Oil supply pressure and temperature were fixed at 140kPa and 40ºC, respectively.

Hydrodynamic pressure distribution and minimum film thickness.

Hydrodynamic pressure profiles at the mid-plane of the bearing are presented on Fig. 4(a) for a fixed rotational speed (2000rpm) and five different load values (2, 4, 6, 8, and 10kN), and on Fig. 4(b) for fixed load (10kN) and two values of rotational speed (1000 and 4000 rpm)

Pressure is generated hydrodynamically at the convergent portion of the film. The pressure buildup zone is located mainly between the upstream and the downstream groove. That is why this zone is usually called the loaded lobe of the bearing. As load increases the maximum pressure tends to increase in a nearly linear form, while the pressure buildup zone tends to be smaller. The peak of the pressure profile is located near the zone of minimum film thickness. After this zone the geometry of the film becomes divergent and film rupture takes place. Here the pressure starts being sub-ambient, reaching zero gradually. As load increases (or rotational speed decreases), it can be observed at Fig 4 that film rupture tends to occur further upstream.

For instance, it can be seen in Fig. 4(a) that, for the tests with loads of 8 and 10kN film rupture occurred at an angle of less than 150º, while for the 2kN test a negative pressure indicating film rupture was only observed for an angle higher than 210º. These results can be explained observing Fig. 5, which represents the minimum film thickness as a function of applied load and rotational speed. As load increases, the minimum film thickness decreases. For instance, for the lowest speed tests (1000 rpm) there was a decrease of 72% in this factor (from 73µm to 20µm) as load increased from 2 to 10kN. For the highest speed this decrease was only of 48%.

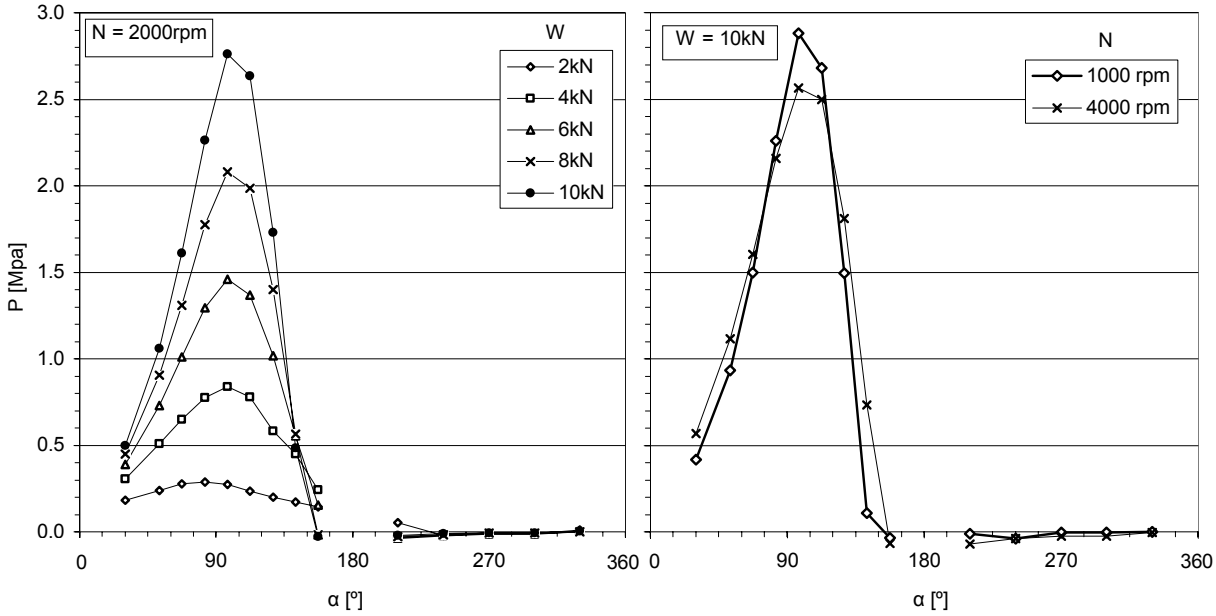

(a) (b)

Fig. 4 – Influence of (a) applied load and (b) rotational speed on the hydrodynamic pressure profile at the mid-plane of the bush-film interface.

For this bearing geometry the decrease in minimum film thickness factor is associated with a decrease in attitude angle. This means that the minimum film thickness zone (and therefore the rupture zone) is located further upstream. Additionally, due to a lower minimum film thickness (Fig. 5), the film geometry becomes more intensely divergent, being subject to an earlier film rupture. Reformation occurs in the convergent zone of the film or in the vicinity of oil grooves. The film reformation border cannot be easily located experimentally, unless transparent glass bushes were used.

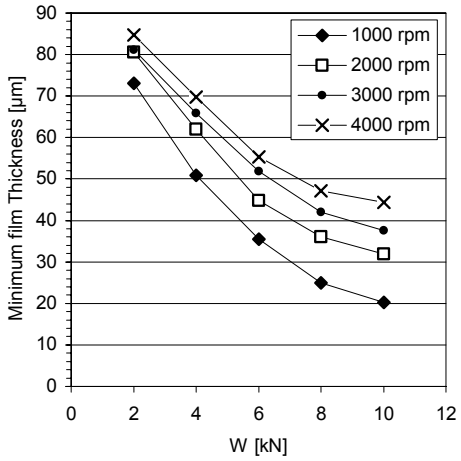

Fig. 5 – Influence of applied load and rotational speed on minimum film thickness.

The increase in shaft speed increases the bearing load carrying capacity. In other words, if the load is kept constant, the minimum film thickness is higher when rotational speed is higher. Under these conditions, increasing rotational speed yields smaller pressure peaks and wider pressure buildup zones as seen in Fig. 4(b).

Oil flowrate

Figure 6 depicts the influence of rotational speed and applied load on oil flowrate. Shaft speed clearly affects this oil flowrate, as the *Couette* component of the oil flow inside the bearing directly depends on shaft speed. When shaft speed increased from 1000rpm to 4000rpm oil flowrate increased by 45% and 68% for 2 kN and 10kN loads, respectively. The observed increase is nearly linear.

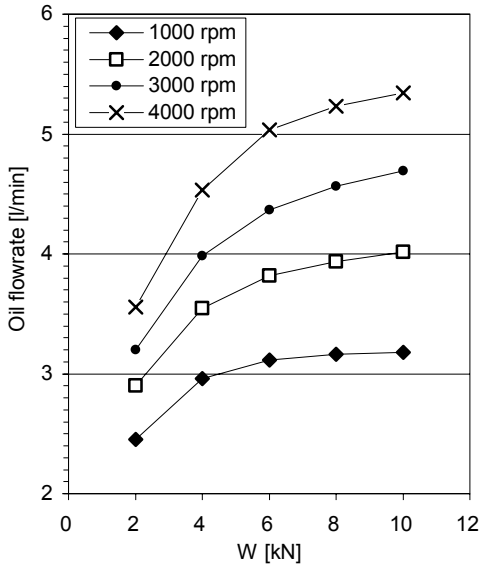

Fig. 6 – Influence of applied load and rotational speed on oil flowrate.

Applied load has also a marked effect on oil flowrate. It can be observed that the increase in applied load from 2kN to 10kN yielded increases in oil flowrate of 30% and 50% at 1000rpm and 4000rpm, respectively. The increase in flowrate is high under low loads loosing intensity as load increases. Moreover, for the highest eccentricity cases (low speed – high load) oil flowrate seems to have stopped to increase with increasing load. Therefore, it is clear that shaft eccentricity plays an important role on oil flowrate. Under low loads (low eccentricity) the pressure gradients inside the bearing are weak and only a small amount of oil leaks to the bearing sides. As load increases, the hydrodynamic pressure field at the loaded lobe becomes more intense, promoting oil leakage and subsequent renewal. Additionally, as load increases the pressure buildup zone moves upstream, away from the downstream groove region, facilitating oil supply. These two factors should contribute to a substantial increase in oil supply at the downstream groove. On the other hand, as load increases, the pressure buildup zone gets closer to this groove, making more difficult the entry of fresh oil through the upstream groove. Oil flowrate is a parameter of great relevance for the analysis of the temperature field inside the bearing, which will be carried in the next section.

Temperature measurements

Figure 7 represents the temperature profiles at the mid-plane of the bush-film interface for three different rotational speeds. Results for five different load values are displayed in each plot.

Increasing rotational speed globally rises the temperature level inside the bearing. This is due to the increase in the shear rate that is associated with the increase of velocity gradients across the film thickness.

Under low loads the maximum temperature occurs in the unloaded lobe of the bearing. Here the heat generation is not concentrated at the vicinity of the position of minimum film thickness as in the high load cases, being more distributed circumferentially because the shaft is almost concentric with the bush. Also the oil flowrate is low. As load increases, the temperature at the loaded lobe tends to increase, due to a decrease in minimum film thickness which promotes the increase of heat generation near the zone of minimum film thickness. This causes a temperature rise concentrated around this area. As explained earlier, there is also an increase in fresh oil entry at the downstream groove that tends to lower the temperature in the unloaded lobe. For instance, for the 4000rpm tests the maximum temperature in the loaded lobe increased by 7.8ºC, while in the unloaded lobe decreased by 4.7ºC as load increased from 2k**N** to 10kN. Above a certain value of load, the maximum value of temperature changes from the unloaded lobe to the loaded lobe of the bearing.

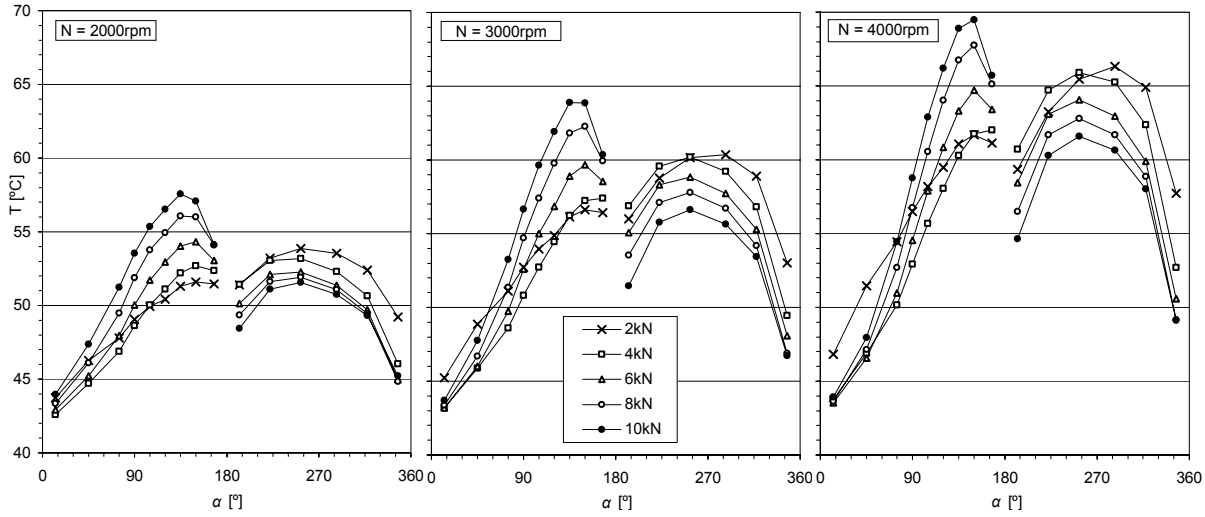

(a) (b) (c)

Fig. 7 – Temperature profile at the mid-plane of the bush-film interface for (a) N=2000 rpm, (b) N=3000 and (c) 4000 rpm

Figure 8 depicts the temperature drop across each groove, i.e. the difference between the temperatures measured by the thermocouples that are located upstream and downstream of each groove, respectively (in reality, these thermocouples are a few degrees away from the edges of the grooves). This is a relative measure of the cooling effect of each groove.

It can be concluded from Fig. 8(a) that the cooling effect of the downstream groove is almost negligible for loads below 4kN, with temperature drops across the groove of less than 1.8ºC, but it gains importance as load increases, with temperature drops as high as 11.1ºC for 10kN. On the contrary, as load increases the cooling effect of the upstream groove loses importance: It can be seen in Fig. 8(b) that the higher the applied load, the lower the temperature fall across this groove. The temperature drop across this groove was as high as 10.9ºC in the

lowest eccentricity test (4000rpm, 2kN), while the temperature across the groove did not change significantly in the test with the highest eccentricity (1000rpm, 10kN).

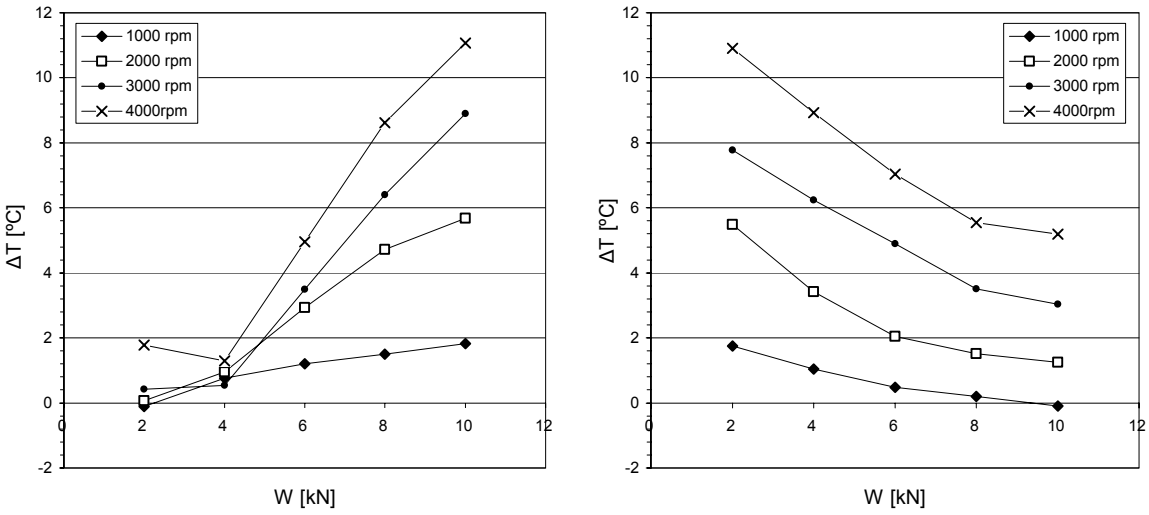

(a) (b)

Fig. 8 – Temperature drop across (a) the downstream groove and (b) the upstream groove.

Shaft Temperature (T_{Shaft}) and oil outlet temperature (T_{out}) do not seem to be affected by load, but they are significantly affected by rotational speed, as shown in Fig. 9. Under low loads T_{Shaft} is between 1ºC and 3ºC lower than the maximum bush temperature, which is located at the unloaded lobe. Under high loads, T_{Shaft} is up to 6.3ºC lower than the maximum bush temperature, which occurs in the loaded lobe (see Fig. 7)

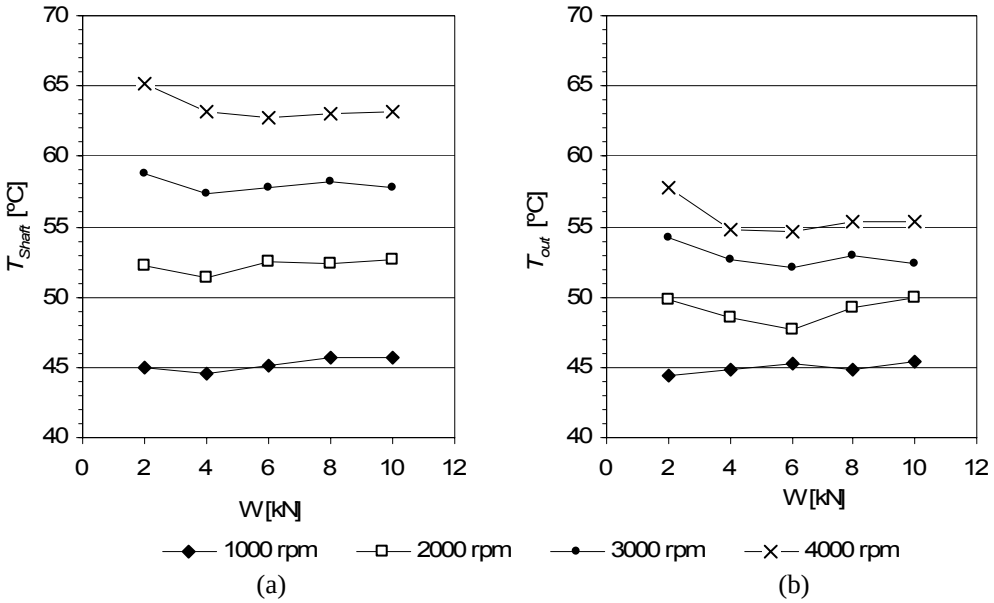

(a) (b)

Fig. 9 – Influence of the operating conditions on (a) Shaft Temperature and (b) oil outlet temperature.

CONCLUSIONS

An experimental investigation on the thermal behavior of a twin axial groove journal bearing has been carried out. In order to address the current lack of experimental data on this issue, a wide range of operating conditions was tested. Results for hydrodynamic pressure,

temperature profiles at the oil-bush and oil-shaft interfaces, oil outlet temperature, oil flowrate and minimum film thickness have been presented and discussed.

Increasing shaft rotational speed resulted in a global increase on bearing temperature. A nearly linear increase of shaft temperature, maximum bush temperature and oil flowrate was observed with increasing speed.

An increase in applied load caused a temperature increase in the loaded lobe and a temperature decrease in the unloaded lobe, but did not seem to affect significantly shaft temperature and oil outlet temperature. Oil flowrate increased with increasing speed and load, but seemed to stabilize for the highest eccentricity cases.

The cooling effect of each supply groove was found to be dependent on the operating conditions. For instance, the cooling effect of the downstream groove was found to be negligible under low load conditions, having a notorious effect on lowering the bearing temperature in the region at high loads. On the other hand, as load increased, the cooling effect of the upstream groove decreased.

ACKNOWLEDGEMENTS

The present work was undertaken under the project POCTI/39202/EME/2001, funded by *FCT - Fundação para a Ciência e a Tecnologia* (Portugal) and the European Union fund *FEDER*. The work has been carried out at the *Laboratoire de Mécanique des Solides*, URM CNRS 6610, University of Poitiers (France). The authors greatly acknowledge the support of these institutions.

REFERENCES

Boncompain R ., Fillon M. and Frene J., 1986, “Analysis of thermal effects in hydrodynamic bearings”, ASME Journal of Tribology, vol. 108, p. 219-224.

Mitsui, J. A,, 1987, “Study of Thermohydrodynamic lubrication in a circular journal bearing”. Tribology Int., 20, p. 331-341.

Pierre, I. and Fillon, M., 2000, “Influence of geometric parameters and operating conditions on the Thermohydrodynamic behaviour of plain journal bearings”. Proc. Instn Mech. Engrs, Part J: J. Engineering Tribology, 214, P. 445-457.

Knight J. D., and Ghadimi P., 1992, “Effects of modified Effective lenght models of the rupture zone on the analysis of a fluid journal bearings”, STLE Tribology Transactions, Vol.35, pp 29-36.

Ma M. T., and Taylor C. M., 1994, “Prediction of temperature fade in cavitation region of two-lobe journal bearings”, Proc. ImechE, Part J, Vol 208, pp. 133-139

Lund J. W., and Tonnesen J., 1984, “An approximate analysis of the temperature conditions in a journal bearing. Part II: Application”, ASME Journal of Tribology, Vol. 106, pp. 237–245.

Fitzgerald M. K., and Neal P. B., 1992, “Temperature distributions and heat transfer in journal bearings”, ASME Journal of Tribology, Vol. 114, pp. 122–130.

Ma M. T., and Taylor C. M., 1995, “Effects of Oil feed Temperature on the Performance of an Elliptical Bore Bearing”, Lubricants and Lubrication – Proceedings of the 21st Leeds-Lyon

Symposium on Tribology held at the Institute of Tribology, University of Leeds, U.K., 6th-9th September 1994, pp 143–151.

Ferron, J., Frêne, J., and Boncompain, R., 1983, "A Study of the Thermohydrodynamic Performance of a Plain Journal Bearing. Comparison Between Theory and Experiments," ASME J. Lubr. Technol., 105, pp. 422–428.

Bouyer, J., and Fillon, M., 2002 “An Experimental Analysis of Misalignment Effects on Hydrodynamic Plain Journal Bearing Performances”, ASME Journal of Tribology, Vol. 124, pp. 313–319.